JACS
JOURNAL OF THE AMERICAN CHEMICAL SOCIETY

Article

pubs.acs.org/JACS

Postsynthetically Modified Covalent Organic Frameworks for Efficient and Effective Mercury Removal

Qi Sun,[†] Briana Aguila,[†] Jason Perman,[†] Lyndsey D. Earl,[‡] Carter W. Abney,[‡] Yuchuan Cheng,[§] Hao Wei,[∥] Nicholas Nguyen,[†] Lukasz Wojtas,[†] and Shengqian Ma*[,†]

[†]Department of Chemistry, University of South Florida, 4202 East Fowler Avenue, Tampa, Florida 33620, United States

[‡]Chemical Sciences Division, Oak Ridge National Laboratory, P.O. Box 2008, Oak Ridge, Tennessee 37831, United States

[§]Zhejiang Key Laboratory of Additive Manufacturing Materials, Ningbo Institute of Materials Technology and Engineering, Chinese Academy of Sciences, 1219 Zhongguan West Road, Ningbo, Zhejiang 315201, China

[∥]School of Electronic Information and Electrical Engineering, Shanghai Jiao Tong University, Shanghai 200240, China

Supporting Information

ABSTRACT: A key challenge in environmental remediation is the design of adsorbents bearing an abundance of accessible chelating sites with high affinity, to achieve both rapid uptake and high capacity for the contaminants. Herein, we demonstrate how two-dimensional covalent organic frameworks (COFs) with well-defined mesopore structures display the right combination of properties to serve as a scaffold for decorating coordination sites to create ideal adsorbents. The proof-of-concept design is illustrated by modifying sulfur derivatives on a newly designed vinyl-functionalized mesoporous COF (COF-V) via thiol−ene "click" reaction. Representatively, the material (COF-S-SH) synthesized by treating COF-V with 1,2-ethanedithiol exhibits high efficiency in removing mercury from aqueous solutions and the air, affording Hg^{2+} and Hg^0 capacities of 1350 and 863 mg g^{-1}, respectively, surpassing all those of thiol and thioether functionalized materials reported thus far. More significantly, COF-S-SH demonstrates an ultrahigh distribution coefficient value (K_d) of 2.3×10^9 mL g^{-1}, which allows it to rapidly reduce the Hg^{2+} concentration from 5 ppm to less than 0.1 ppb, well below the acceptable limit in drinking water (2 ppb). We attribute the impressive performance to the synergistic effects arising from densely populated chelating groups with a strong binding ability within ordered mesopores that allow rapid diffusion of mercury species throughout the material. X-ray absorption fine structure (XAFS) spectroscopic studies revealed that each Hg is bound exclusively by two S via intramolecular cooperativity in COF-S-SH, further interpreting its excellent affinity. The results presented here thus reveal the exceptional potential of COFs for high-performance environmental remediation.

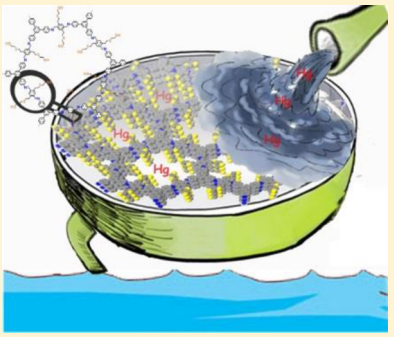

INTRODUCTION

Environmental pollution is of growing worldwide concern, and it is imperative to remove natural and anthropogenic toxic contaminants from the water and air,[1] especially heavy-metal species which pose serious health effects.[2] Among all the techniques trialed for this purpose, adsorption holds considerable promise.[3,4] To achieve high uptake capacity, fast kinetics, and excellent selectivity, the use of complexing functionalities has come into play to combat heavy-metal pollution.[5] Numerous adsorbents have been developed based on the covalent grafting of coordination groups to the surface of porous materials such as silica gel and clay. Nonetheless, only a fraction of the surface-bound ligands is found to interact with the targeted metal ions due to their small and irregular pore structures, limiting the access of contaminants to the grafted ligands and thus compromising metal binding capacity.[6] Mesoporous molecular sieves were alternatively used to alleviate this issue due to their large uniform pore structures, which preclude pore blockage by the grafted species and thereby facilitate the interaction between metal ions and binding sites.[7] However, the limited amount of silanol groups on the surface inevitably diminishes the population density of chelating sites, thus resulting in low saturation capacity and affinity. Considering these weaknesses associated with existing adsorbents, it is therefore necessary to develop new types of materials that show greater potential in remediation technology.

Covalent organic frameworks (COFs)[8] have emerged as a type of porous material with significant prospects for addressing current challenges pertinent to energy and environmental sustainability, including gas adsorption,[9] optoelectronics,[10] catalysis,[11] proton conduction,[12] and many more.[13] The tunable nature of COFs may also be beneficial in mitigating environmental problems caused by toxic heavy metals. We reason that such materials have the right combination of properties that give them potential as excellent sorbents for environmental remediation, in particular, two-dimensional COFs. These advantages, leading to enhanced binding affinity

Received: December 15, 2016
Published: February 13, 2017

DOI: 10.1021/jacs.6b12885
J. Am. Chem. Soc. 2017, 139, 2786−2793

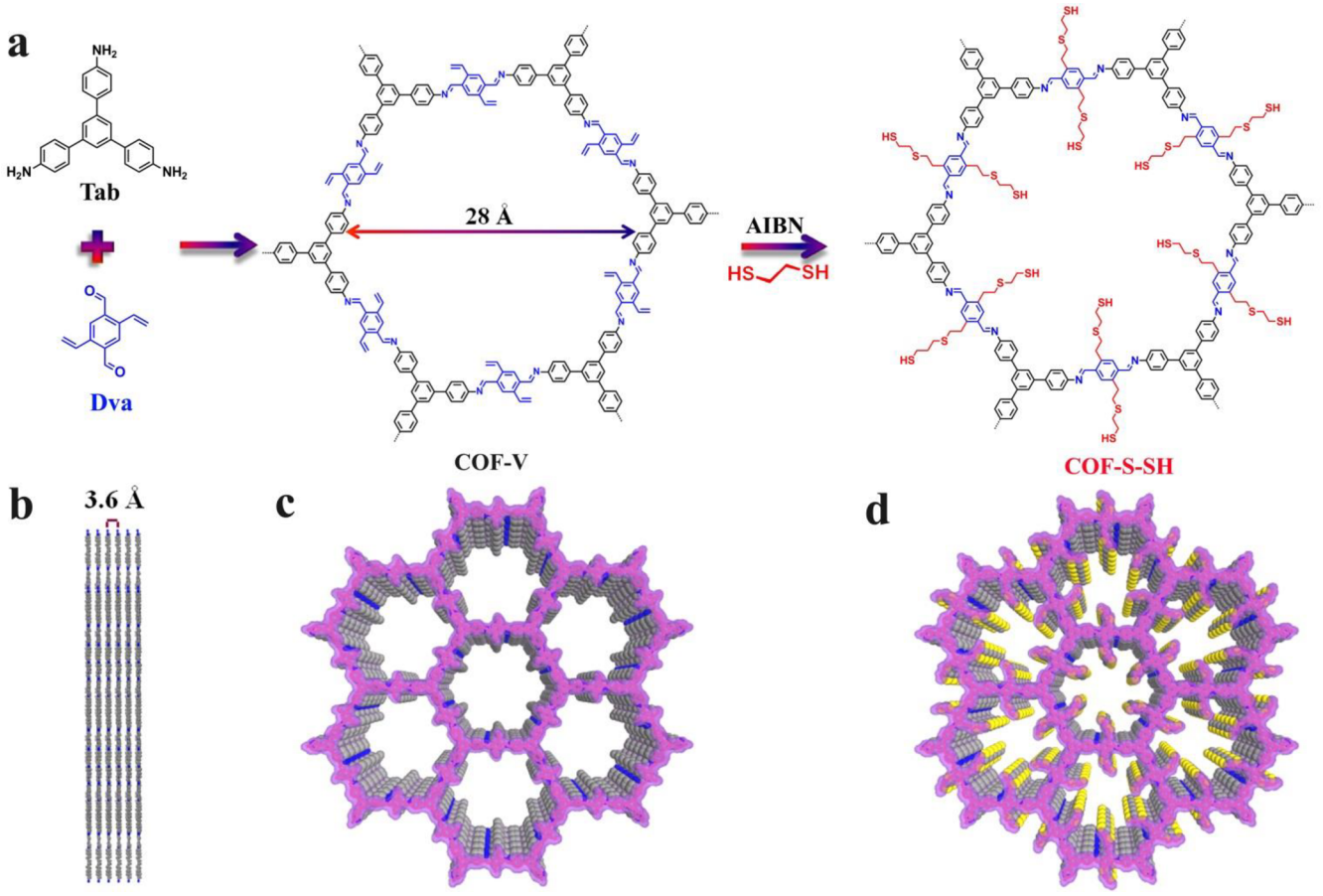

Figure 1. (a) Synthetic scheme of COF-V through the condensation of Tab (black) and Dva (blue) and representative channel-wall engineering by thiol−ene reaction with (COF-S-SH). (b, c) Graphic view of the slipped AA stacking structure of COF-V (blue, N; gray, C; hydrogen is omitted for clarity). (d) Graphic view of COF-S-SH (blue, N; gray, C; yellow, S; hydrogen is omitted for clarity).

and uptake capacity, include (1) a highly tunable molecular design, allowing for atomically precise integration of building blocks into porous structures; (2) crystallinity, offering a strategy to position functional groups in a highly controlled and predictable manner; and (3) the nearly eclipsed and ordered π-columnar structures of most 2D COFs, enabling the functional groups to be fully accessible and in close proximity with each other to facilitate their cooperation. Despite the success in obtaining functionally diverse COFs via direct synthesis, for example, a thioether based 2D COF developed for sensing applications,[4d] the scope of functional groups within the pores of the COFs has remained relatively limited due to the fact that not all functional groups are compatible with or stable to the conditions for the COFs synthesis.

In order to impart specific functionality on the COFs, we designed a vinyl-functionalized monomer (2,5-divinylterephthalaldehyde) where the vinyl groups can remain intact during the COF synthesis, thus allowing for further chemical modifications.[14] In addition, it has been proven that COFs constructed with imine bonds can withstand a wide range of conditions.[15] As such, the newly designed vinyl-functionalized COF (COF-V), synthesized by the condensation between 2,5-divinylterephthalaldehyde and 1,3,5-tris(4-aminophenyl)-benzene, is attractive because of its stability and potential for versatile modification. In view of toxic metal species, mercury and other soft heavy-metal species, such as lead, present a serious environmental concern and constitute a threat to public health. For example, mercury is inclined to transform to the potent neurotoxin methylmercury, which can be bioaccumulated and biomagnified in aquatic food chains. In this sense, effective capture and removal of them is mandatory and has attracted considerable interest. Considering the extraordinary binding ability of sulfur derivatives with soft heavy-metal species, such as mercury, and high throughput of thiol−ene transformations, a series of thiol compounds with different flexibility and sulfur species density were chosen to demonstrate the proof-of-concept. The resultant sulfur-based chelating-group-laced COFs, with retained crystallinity and porosity, are capable of effective mercury removal from both aqueous solutions and the gas phase with outstanding uptake capacity [up to about 1350 mg g^{-1} (with an equilibrium concentration of 110 ppm) and 863 mg g^{-1} for Hg^{2+} and Hg^0, respectively] and can rapidly diminish the Hg^{2+} concentration down to 0.1 ppb level even with a high concentration of competing ions present. The synergistic effects of densely populated yet highly accessible chelating groups on the ordered one-dimensional meso-channels afford COF-S-SH with the highest mercury uptake capacity known among thiol and thioether functionalized materials, placing it within striking distance of the all-time mercury uptake record.[19] Our studies therefore lay a foundation for developing COFs as a promising type of host material for the deployment of adsorbents that circumvent the issues of buried chelating sites and a low degree of functionalization encountered in conventional materials.

DOI: 10.1021/jacs.6b12885
J. Am. Chem. Soc. 2017, 139, 2786−2793

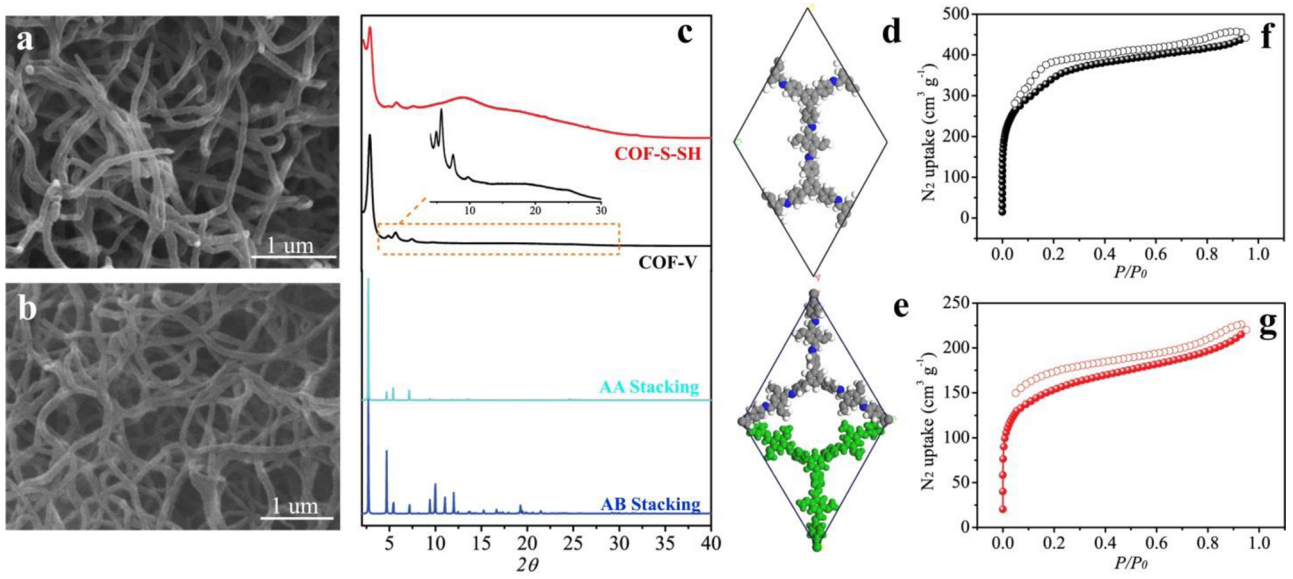

Figure 2. (a, b) SEM images for COF-V and COF-S-SH, respectively. (c) PXRD profiles. (d) Unit cell of the AA stacking mode of COF-V (N, blue; C, gray; H, white). (e) Unit cell of the AB stacking mode of COF-V (N, blue; C, gray; H, white; green, a further layer). (f, g) Nitrogen-sorption isotherm curves measured at 77 K for COF-V and COF-S-SH, respectively.

RESULTS AND DISCUSSION

Material Preparation, Physiochemical Characterization, and Local Structure Analysis. Herein, COF-V was synthesized via an imine condensation reaction between 2,5-divinylterephthalaldehyde (Dva) and 1,3,5-tris(4-aminophenyl)benzene (Tab) using 1:1 *n*-butylalcohol/1,2-dichlorobenzene as the solvent in the presence of 6 M acetic acid at 100 °C for 3 days (Figure 1). The Fourier transform infrared (FT-IR) spectrum of the COF-V was compared with that of the precursors and showed the appearance of the characteristic peak for C═N at 1606 cm^{-1} with the concomitant disappearance of the aldehydic C−H (2875 and 2779 cm^{-1}) and C═O (1676 cm^{-1}) stretching vibrations of Dva and the N−H (3430 and 3355 cm^{-1}) stretching vibrations of Tab, thus indicating the condensation occurrence (Figure S1).[15] The morphology of the COF-V was examined by scanning electron microscopy (SEM) and transmission electron microscopy (TEM), which showed a large quantity of uniform nanofibers with diameter of about 80 nm and lengths up to tens of micrometers, thus implying its phase purity (Figures 2a and S2).

To analyze the structure of the obtained material, powder X-ray diffraction (PXRD) and theoretical simulation experiments were conducted. In the experimental PXRD profile of COF-V, a strong peak at 2.72° together with some relatively weaker peaks at 4.74, 5.48, 7.27, 9.54, and 24.9° were observed, which were assigned to (100), (110), (200), (210), (220), and (001) diffractions (Figure 2c). To elucidate the constitution of the framework, we constructed a structural model using Materials Studio. Pawley refinements of the PXRD patterns were carried out for full profile fitting against the proposed model of AA packing, which resulted in good agreement factors (R_{WP} = 1.7 after convergence) and reasonable profile differences (Figure S3 and Table S1). We interpreted the refinement data to show that COF-V has one-dimensional channels, with a diameter of 28 Å, along the *c*-axis and that the layers stack with an interlayer distance of 3.6 Å. The porosity and specific surface area were determined to be 1152 $m^2\ g^{-1}$ from N_2 sorption isotherms at 77 K. DFT fitting of the adsorption branches showed pore size distributions mainly at 2.8 nm in agreement with that of the proposed model (Figure S4). The framework of COF-V is stable in ambient air and retains its crystallinity after soaking in a variety of organic solvents and water, as well as both acid (1 M HCl) and base (2 M NaOH) aqueous solutions (Figure S5).

Intrigued by its high crystallinity, mesoporous channels, and chemical stability, we developed COF-V into heavy-metal adsorbent materials by anchoring sulfur derivatives (thiol and/or thioether) onto the channel walls using thiol−ene "click" reaction between thiol compounds and the vinyl groups in COF-V with the assistance of azobis(isobutyronitrile) (AIBN). The material obtained by the treatment of COF-V and 1,2-ethanedithiol (COF-S-SH) was taken as a representative sample for full illustration. The PXRD pattern of COF-S-SH exhibited a diffraction pattern comparable to that of COF-V but with broadened peak widths (Figure 2c). We attributed the broad peak widths to the large numbers of flexible chains in the pores of the COF, thus slightly distorting the long-range order of the crystalline material.[16] Nitrogen sorption measurements revealed that COF-S-SH still gave a BET surface area as high as 546 $m^2\ g^{-1}$, which is indicative of pore accessibility after modification. SEM and TEM images of COF-S-SH also exhibited uniform nanofibers, indicating that no noticeable morphological changes occurred following chemical modification as compared with that of COF-V (Figures 2b and S6). The successful grafting of thiol and thioether groups onto the COF-V was confirmed by X-ray photoelectron spectroscopy (XPS), FT-IR, solid-state ^{13}C NMR studies, and elemental analysis. The XPS spectrum of COF-S-SH revealed the sulfur signal at a binding energy of 163.9 eV, verifying the postsynthetic modification (Figure S7).[17] In addition, the FT-IR spectrum of the COF-S-SH showed the characteristic band of S−H at 2552 cm^{-1} compared with that of pristine COF-V, confirming the existence of free-standing thiol groups (Figure S8).[17] The high throughput of the thio-ene transformation was determined by the disappearance of the peaks assigned to the vinyl groups at around 110 ppm in the ^{13}C MAS NMR spectrum of COF-S-SH and the concomitant emergence of strong peaks at 42.1

DOI: 10.1021/jacs.6b12885
J. Am. Chem. Soc. 2017, 139, 2786−2793

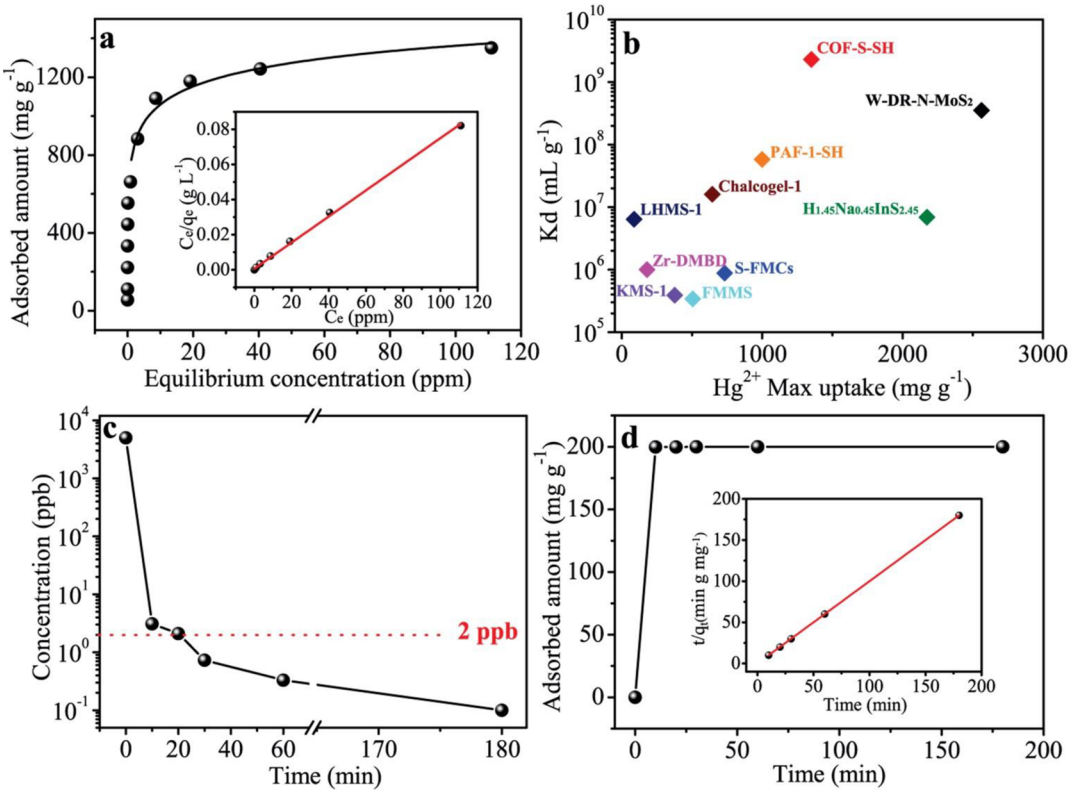

Figure 3. (a) Hg^{2+} adsorption isotherm for COF-S-SH. Inset shows the linear regression by fitting the equilibrium data with the Langmuir adsorption model. (b) Comparison of Hg^{2+} saturation uptake amount and K_d value for COF-S-SH with those of other benchmark porous materials: PAF-1-SH (ref 17); LHMS-1 (ref 19a); FMMS (ref 19b); Chalcogel-1 (ref 19c); S-FMC-900 (ref 19d); Zr-DMBD (ref 19e); W-DR-N-MoS_2 (ref 19f); $H_{1.45}Na_{0.45}InS_{2.45}$ (ref 19g); KMS-1 (ref 19h). (c) Hg^{2+} sorption kinetics of COF-S-SH with Hg^{2+} initial concentration of 5 ppm at a V/m ratio of 46500 mL g^{-1}. (d) Adsorption curve of Hg^{2+} versus contact time in aqueous solution using COF-S-SH. Inset shows the pseudo-second-order kinetic plot for the adsorption.

ppm ascribed to the alkyl C species (Figure S9).[18] Furthermore, elemental analysis of COF-S-SH revealed sulfur content of 20.9 wt % that corresponds to 6.53 mmol g^{-1} sulfur species. This suggests that more than 90% of the vinyl groups reacted with 1,2-ethanedithiol. These results are consistent with the ^{13}C MAS NMR analysis. On the basis of the above, we can conclude that a high density of sulfur species was incorporated without significantly altering the crystalline structure of COF-V.

Hg^{2+} Sorption Studies. After confirming the porosity, structural integrity, and high density of chelating sites of COF-S-SH, we examined its ability to capture Hg^{2+} from aqueous solutions. To assess the overall capacity of COF-S-SH for Hg^{2+}, equilibrium values were collected after exposure to Hg^{2+} aqueous solutions with initial concentrations in the range of 25−700 ppm. As shown in Figure 3a, COF-S-SH exhibits a very steep adsorption profile for Hg^{2+}, approaching the ideal type-I isotherm shape, thus indicating that COF-S-SH has a very strong affinity for Hg^{2+}. The equilibrium adsorption isotherm data was well-fitted with the Langmuir model, yielding a correlation coefficient as high as 0.998. Remarkably, COF-S-SH was determined to have a capacity of about 1350 mg of Hg^{2+} per gram of adsorbent, surpassing all previously reported thiol and/or thioether functionalized materials for mercury decontamination and outperforming most of the layered metal sulfide adsorbents (Figure 3b, Table S2).[19] Specifically, it is 2.5 times better than the best sorption obtained with mesoporous silica,[19b] almost doubling the sulfur-functionalized mesoporous carbon (S-FMC),[19d] 7 times higher than thiol laced MOF,[19e] 1.5 times higher than the best MOF (BioMOF),[19i] and 30% higher than the benchmark mercury sorbent material PAF-1-SH.[17] Such an outstanding saturation mercury uptake capacity can be attributed to the tremendous affinity together with a large number of highly accessible sulfur species that are well-dispersed throughout the channel surface of COF-S-SH. Based on the previously determined sulfur content, the calculated Hg capacity for COF-S-SH would equal 1320 mg Hg per gram of adsorbent, which means virtually all of the sulfur-based functionality in the COF-S-SH is available for binding Hg. The slight deviation between the experimental and calculated uptake capacities could presumably be attributed to the conjugated COF host, which is capable of interaction with Hg^{2+} from a $Hg^{2+}-\pi$ interaction.[20] Accordingly, it is revealed that COF-V afforded a mercury saturation adsorption capacity of 147 mg g^{-1} treated under the same conditions as Figure 3a with an initial Hg^{2+} concentration of 700 ppm. It is noteworthy that the PXRD pattern and SEM image (Figure S10) suggest the retention of both crystallinity and the integrity of the material after the sorption process. More significantly, COF-S-SH can readily be regenerated by treating it with 1,2-ethanedithiol, and it was demonstrated to retain its mercury uptake capacity for at least four consecutive cycles, affording a value of 1280 mg g^{-1} (Figure S11).

In addition to the high Hg^{2+} uptake capacity, time-course adsorption measurements further indicated that Hg^{2+} capture by COF-S-SH is kinetically efficient (Figure 3c). It can attain 99.94% of the adsorption capacity at equilibrium within 10 min and was able to reduce a heavily contaminated water (Hg^{2+} concentration of 5 ppm) to 0.73 ppb, far below the acceptable

DOI: 10.1021/jacs.6b12885
J. Am. Chem. Soc. 2017, 139, 2786−2793

limit of 2 ppb for drinking water within 30 min of contact in the presence of a very small amount of adsorbent (V/m at 46500 mL g^{-1}). Prolonging the contact time to 3 h, the Hg^{2+} concentration was reduced below the detection limit of ICP-MS for Hg (0.1 ppb). The adsorption kinetic process was well-fitted with the pseudo-second-order kinetic model expressed as

$$\frac{t}{q_t} = \frac{1}{k_2 q_e^2} + \frac{t}{q_e}$$

where k_2 (g mg^{-1} min^{-1}) is the pseudo-second-order rate constant of adsorption, q_t (mg g^{-1}) is the amount of Hg^{2+} adsorbed at time t (min), and q_e (mg g^{-1}) is the amount of Hg^{2+} adsorbed at equilibrium (Figure 3d). The initial adsorption rate, h ($k_2 q_e^2$), has been widely used for evaluation of the adsorption rates. Accordingly, COF-S-SH gives an h value as high as 143 mg g^{-1} min^{-1}, far exceeding that reported for a series of benchmark materials, for example, PAF-1-SH.[17] Such extraordinarily fast kinetics observed for COF-S-SH can be ascribed to the high concentration of chelating groups together with well-defined pore channels adequate to facilitate the diffusion of Hg^{2+} ions. These results underscore the superiority of the utilization of COFs as promising candidates in accomplishing mercury removal from water.

Investigation of Hg^{2+} Binding Interaction. The outstanding performance of COF-S-SH in mercury sequestration can be traced to the remarkable binding interactions between the Hg and sulfur species in COF-S-SH, which have been elucidated by XPS, FT-IR, and Raman spectroscopy studies. Mercury inclusion within COF-S-SH was confirmed by the appearance of Hg^{2+} XPS signals at 101.4 and 105.4 eV assigned to the Hg $4f_{7/2}$and Hg $4f_{5/2}$, respectively. The strong binding interactions between the Hg^{2+} and S species in Hg@COF-S-SH were observed from the S 2p XPS spectra, which showed a 0.6 eV shift for the S binding energy in Hg@COF-S-SH compared to that of COF-S-SH (Figure S12). Furthermore, the absence of the characteristic S−H stretching mode at 2552 cm^{-1} in the IR spectrum of COF-S-SH upon saturation with Hg^{2+} (Hg@COF-S-SH) verifies the interactions between S−H groups and Hg^{2+} (Figure S13). Moreover, the peaks in the Raman spectrum of Hg@COF-S-SH at 391 and 408 cm^{-1}, attributed to the Hg−S stretching vibrations (ν_{as} = 408 cm^{-1}, ν_s = 391 cm^{-1}), confirmed the coordination between S and Hg species (Figure S14).[21]

It is noteworthy that the mercury-capture performance of COF-S-SH is superior to that exhibited by state-of-the-art thiol and/or thioether functionalized adsorbents. Besides the apparent accessibility of the densely populated chelating groups, to gain more insight into this unexpected performance, we gauged the importance of flexibility and type of sulfur species in the chelating groups. To test flexibility, we modified COF-V with a more rigid molecule, benzene-1,4-dithiol, making COF-S-Ph-SH (S content 10.2 wt %, Figures S15–18). To test the sulfur species, we modified COF-V with ethanethiol to form COF-S-Et, which only contains the thioether group (S content 8.9 wt %, Figures S19–S22). As seen in Figure 4, both COF-S-Ph-SH and COF-S-Et are inferior to COF-S-SH in terms of removal kinetics and efficiency after exposure to Hg^{2+} aqueous solutions with the same initial concentration of 5 ppm. Specifically, the remaining mercury concentrations were 1.3 and 22.0 ppb, respectively. The large disparity in removal efficiency between COF-S-SH and COF-S-Ph-SH is mainly due to the highly flexible chelating arms of

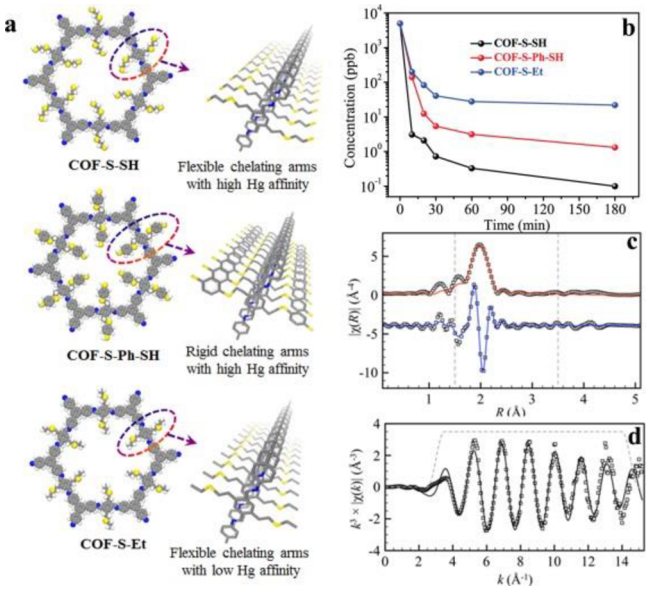

Figure 4. (a) Open structures of the adsorbents and the chelating arms on the channel walls (S, yellow; N, blue; C, gray). (b) Hg^{2+} sorption kinetics over various adsorbents with Hg^{2+} initial concentration of 5 ppm. (c) Fourier transform of the Hg L_{III}-edge EXAFS spectrum of COF-S-SH in *R*-space. The magnitude of the Fourier transform is fit by a red line; the real component is fit with a blue line. (d) Accompanying k^3-weighted $\chi(k)$ data and fit (black line).

COF-S-SH that can be arranged in different conformations, ready for metal ions to adopt a favorable form, thereby increasing the affinity, which is reminiscent of that seen in biological systems and protein receptors.[22] With respect to COF-S-Et, due to thioether having a lower affinity for mercury compared with the thiol group, the removal efficiency is inferior to that of thiol-contained adsorbents, COF-S-SH and COF-S-Ph-SH, as demonstrated by its higher residual mercury concentration (22.0 ppb).

To gain more insight into the coordination environment of mercury in the three thiol and/or thioether-functionalized COF materials, we employed X-ray absorption fine structure (XAFS) spectroscopy collected at the Hg L_{III}-absorption edge (12.284 keV). Given that the mercury loading in the adsorbents affects the coordination form, we treated these COFs with different volumes of mercury aqueous solution (initial concentration of 20 ppm) to ensure that the S/Hg ratio was around 5 in the resultant mercury included materials.[7b] A representative fit of the extended XAFS (EXAFS) data collected for COF-S-SH is shown in Figure 4c, with other fits provided in Figures S23–S25. In contrast to previous EXAFS data collected on thiol-functionalized mesoporous silica adsorbents, high-quality fits for all adsorbents were only obtainable using Hg−S scattering paths, and no Hg−O contributions were observed. This reveals that each Hg was bound exclusively by two S rather than through −Hg−O−Hg− layering[23,24] or formation of terminal Hg−OH species[19b] and confirms the adsorption of Hg by the COF materials rather than precipitation as HgO.

Analysis of the fitted data also reveals for COF-S-Ph-SH and COF-S-Et that two distinct Hg−S distances are required to obtain an adequate fit of the data. A more quantitative assessment reveals near-equal contributions (56 and 43%) from the two S distances in COF-S-Et, while in COF-S-Ph-SH one S species, the terminal thiol almost certainly predominates in Hg binding (78 and 22%). This suggests steric influences from the

DOI: 10.1021/jacs.6b12885
J. Am. Chem. Soc. 2017, 139, 2786–2793

rigidification of the chelating arm or inclusion of the terminal ethyl restrain the extent of intramolecular cooperativity in Hg binding, rationalizing the relative decrease in Hg adsorption performance discussed above. In contrast, COF-S-SH requires only one Hg−S bond length to fit of the EXAFS spectrum, suggesting the ethylene bridge ideally colocates two S atoms to chelate each Hg atom, thereby giving insight of its outstanding affinity. Additional experimental details and analyses are provided in the Supporting Information.

To evaluate the affinity of adsorbents for mercury, distribution coefficient values (K_d) were thus calculated under conditions identical to those of Figure 4b. Impressively, COF-S-SH demonstrated an ultrahigh K_d value of approximately 2.3×10^9 mL g^{-1} (calculated after reaching equilibrium). This value is the highest for sorbent materials for Hg^{2+} adsorption, representing a 6-fold improvement over the best mercury adsorbent materials reported thus far (3.5×10^8 mL g^{-1} for W-DR-N-MoS_2)[19f] and almost 1 and over 2 orders of magnitude higher than that of COF-S-Ph-SH (1.5×10^8 mL g^{-1}) and COF-S-Et (9.1×10^6 mL g^{-1}), respectively. More importantly, even at pH values of 3 and 10, COF-S-SH still gave rise to K_d values as high as 4.67×10^8 and 1.5×10^8 mL g^{-1}, respectively, thus indicating its superior affinity toward Hg^{2+} over a wide range of pH values. This ability to remove mercury at different pH values and remain stable under these conditions demonstrates great promise for real world applications. On the basis of these results, the following conclusion can be drawn: The synergetic effect from the flexible ligand, framework porosity, and concentrated sulfur species with high affinity for Hg^{2+} account for the extraordinary performance of COF-S-SH.

Selectivity Tests and Hg^0 Vapor Adsorption. To evaluate the ability of COF-S-SH to eliminate Hg^{2+} under realistic conditions, the adsorption kinetic tests were performed using a solution containing Hg^{2+}, Pb^{2+}, Cu^{2+}, Ca^{2+}, Mg^{2+}, Zn^{2+}, and Na^+ ions. COF-S-SH can effectively remove toxic ions Hg^{2+}, Pb^{2+}, and Cu^{2+}, which present a major health hazard. As depicted in Figure 5, the adsorption rates for the ions of Hg^{2+}, Cu^{2+}, and Pb^{2+} were found to be very rapid. Within 10 min, the COF-S-SH achieved >99% removal efficiency for these ions which are below the U.S. Environmental Protection Agency elemental limits for drinking water (Figure S26). Notably, COF-S-SH exhibited negligible capturing capability for various nontoxic competitive ions, such as Ca^{2+}, Mg^{2+}, Zn^{2+}, and Na^+. The unique properties of COF-S-SH stem from its soft sulfur-based chelating groups selective for soft or relatively soft metal ions.

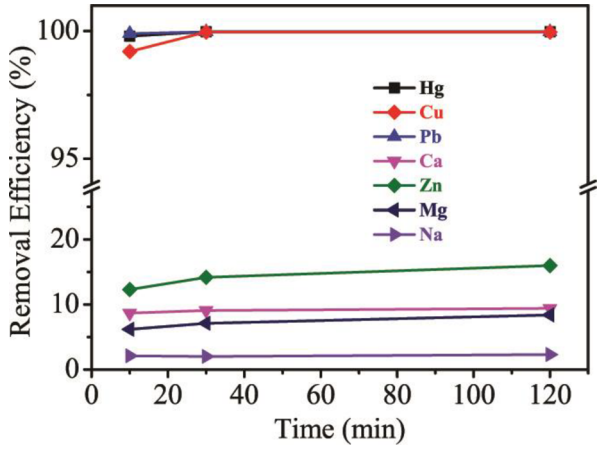

Figure 5. Time-dependent removal efficiency of various ions in the presence of COF-S-SH.

The outstanding mercury removal efficiency of COF-S-SH from solution prompted us to evaluate mercury vapor remediation, an application useful for industrial flue gas detoxification. Mercury vapor control has posed a great challenge for many adsorptive materials, such as activated carbon, because they display low capture capacity at elevated temperatures and suffer from interference of adsorption by other flue gas chemicals.[22] Materials containing sulfur show great promise in terms of adsorption capacity and selectivity; thus, it would be interesting in this regard to study the Hg^0 adsorption properties of COF-S-SH. For the mercury vapor sorption experiment, we modified the approach reported in the literature,[22] where a vial of elemental mercury (liquid, 300 mg) was placed inside a larger vial containing COF-S-SH (20 mg) to create spatial separation. The vial was then immersed in a sand bath and heated at 140 °C. After 3 days of exposure, the adsorption equilibrium was reached as indicated by weight equilibrium. ICP-MS analysis was used to determine the Hg^0 adsorption capacity of the COF-S-SH after it was digested by aqua regia. The equilibrium adsorption capacity value of the COF-S-SH was determined to be 863 mg Hg^0 per gram adsorbent, ranking among the highest of reported materials compared with the benchmark adsorbents listed in Table S3, while under identical conditions, activated carbon (BET = 1011 m^2 g^{-1}) and COF-V gave rise to Hg^0 uptake capacities of 47 and 106 mg g^{-1}, respectively. The highly accessible and densely populated sulfur sites within the COF-S-SH channels contribute to the exceptional mercury vapor adsorption performance, highlighting its great potential applications in Hg^0 vapor control.

CONCLUSION

In conclusion, we have demonstrated the deployment of COFs as an amenable platform for removal of mercury as exemplified by decorating a 2D mesoporous COF with dense and flexible thiol and thioether chelating arms, COF-S-SH. The adsorbent exhibits exceedingly high Hg^{2+} and Hg^0 uptake capacities of 1350 and 863 mg g^{-1}, respectively, a record-high affinity for Hg^{2+} with exceptional distribution coefficient values at a wide pH range from 3 to 10 and extremely fast kinetics for Hg^{2+} adsorption with an unexpected initial adsorption rate as high as 143 mg g^{-1} min^{-1}, surpassing those of all previously reported thiol-functionalized materials. More importantly, COF-S-SH can effectively reduce the Hg^{2+} concentration from 5 ppm to the extremely low level of 0.1 ppb, well below the acceptable limits in drinking water (2 ppb), even in the presence of a high concentration of background metal ions Ca^{2+}, Zn^{2+}, Mg^{2+}, and Na^+. The densely populated yet fully accessible and flexible chelating sites in conjunction with their remarkable affinity for mercury are responsible for the impressive results. Our work thus reveals the enormous potential of COFs as an appealing platform for construction of sorbent materials for environmental remediation, an auspicious function of COFs worthy of further exploration.

EXPERIMENTAL SECTION

Synthesis of COF-V. A Pyrex tube measuring o.d. × i.d. = 9.5 × 7.5 mm^2 was charged with 2,5-divinylterephthalaldehyde (22.3 mg, 0.12 mmol) and 1,3,5-tris(4-aminophenyl)benzene (28.0 mg, 0.08

DOI: 10.1021/jacs.6b12885
J. Am. Chem. Soc. 2017, 139, 2786−2793

mmol) in 1.1 mL of a 5:5:1 v/v/v solution of 1,2-dichlorobenzene/*n*-butylalcohol/6 M aqueous acetic acid. The tube was flash frozen at 77 K (liquid N_2 bath), evacuated, and flame-sealed. Upon sealing, the length of the tube was reduced to ca. 15 cm. The reaction mixture was heated at 100 °C for 3 days to afford a yellow-brown precipitate which was isolated by filtration and washed with anhydrous tetrahydrofuran using Soxhlet extraction for 2 days. The product was dried under vacuum at 50 °C to afford COF-V (39.4 mg, 86%).

Synthesis of COF-S-SH. To the mixture of COF-V (100 mg) and azobis(isobutyronitrile) (AIBN, 10 mg) in a 25 mL Schlenk tube was introduced 1,2-ethanedithiol (4.0 mL) under N_2 atmosphere. After stirring at 80 °C for 48 h, the title product was isolated by filtration, washed by acetone, and dried under vacuum at 50 °C.

■ ASSOCIATED CONTENT

Supporting Information

The Supporting Information is available free of charge on the ACS Publications website at DOI: 10.1021/jacs.6b12885.

Material synthesis; characterization details; IR, SEM, XPS, and NMR; XAFS data collection, fits, and analysis details; supporting figures (PDF)

■ AUTHOR INFORMATION

Corresponding Author

*sqma@usf.edu

ORCID

Jason Perman: 0000-0003-4894-3561

Lyndsey D. Earl: 0000-0003-4359-0197

Shengqian Ma: 0000-0002-1897-7069

Notes

The authors declare no competing financial interest.

■ ACKNOWLEDGMENTS

We acknowledge the University of South Florida for financial support of this work. Work by L.D.E. and C.W.A. was supported financially by the Division of Chemical Sciences, Geosciences, and Biosciences, Office of Basic Energy Sciences, U.S. Department of Energy. This manuscript has been authored by UT-Battelle, LLC under Contract No. DE-AC05-00OR22725 with the U.S. Department of Energy. Use of the Stanford Synchrotron Radiation Lightsource, SLAC National Accelerator Laboratory, is supported by the U.S. Department of Energy, Office of Science, Office of Basic Energy Sciences under Contract No. DE-AC02-76SF00515. We acknowledge the help from Dr. Zachary D. Atlas in the Geochemical Analysis at USF with the ICP-OES/MS experiments.

■ REFERENCES

(1) (a) Zhang, Y.; Wei, S.; Liu, F.; Du, Y.; Liu, S.; Ji, Y.; Yokoi, T.; Tatsumi, T.; Xiao, F.-S. *Nano Today* **2009**, *4*, 135−142. (b) Banerjee, D.; Kim, D.; Schweiger, M. J.; Kruger, A. A.; Thallapally, P. K. *Chem. Soc. Rev.* **2016**, *45*, 2724−2739. (c) Khin, M. M.; Nair, A. S.; Babu, V. J.; Murugan, R.; Ramakrishna, S. *Energy Environ. Sci.* **2012**, *5*, 8075−8109. (d) Tratnyek, P. G.; Johnson, R. L. *Nano Today* **2006**, *1*, 44−48. (e) Alsbaiee, A.; Smith, B. J.; Xiao, L.; Ling, Y.; Helbling, D. E.; Dichtel, W. R. *Nature* **2015**, *529*, 190−194. (f) Byun, J.; Patel, H. A.; Thirion, D.; Yavuz, C. T. *Nat. Commun.* **2016**, *7*, 13377.

(2) (a) Li, X.; Bian, C.; Meng, X.; Xiao, F.-S. *J. Mater. Chem. A* **2016**, *4*, 5999−6005. (b) Ponder, S. M.; Darab, J. G.; Mallouk, T. E. *Environ. Sci. Technol.* **2000**, *34*, 2564−2569. (c) Salt, D. E.; Blaylock, M.; Kumar, N. P. B. A.; Dushenkov, V.; Ensley, B. D.; Chet, I.; Raskin, I. *Bio/Technology* **1995**, *13*, 468−474. (d) Ralston, N. *Nat. Nanotechnol.* **2008**, *3*, 527−528. (e) Johnson, N. C.; Manchester, S.; Sarin, L.; Gao, Y.; Kulaots, I.; Hurt, R. H. *Environ. Sci. Technol.* **2008**, *42*, 5772−5778.

(3) (a) Mulligan, C. N.; Yong, R. N.; Gibbs, B. F. *Eng. Geol.* **2001**, *60*, 193−207. (b) Adewuyi, Y. G. *Environ. Sci. Technol.* **2005**, *39*, 3409−3420. (c) Wang, Q.; Kim, D.; Dionysiou, D. D.; Sorial, G. A.; Timberlake, D. *Environ. Pollut.* **2004**, *131*, 323−336. (d) Aguila, B.; Banerjee, D.; Nie, Z.; Shin, Y.; Ma, S.; Thallapally, P. K. *Chem. Commun.* **2016**, *52*, 5940−5942.

(4) (a) Lee, S.; Barin, G.; Ackerman, C. M.; Muchenditsi, A.; Xu, J.; Reimer, J. A.; Lutsenko, S.; Long, J. R.; Chang, C. J. *J. Am. Chem. Soc.* **2016**, *138*, 7603−7609. (b) Zhong, L.-S.; Hu, J.-S.; Liang, H.-P.; Cao, A.-M.; Song, W.-G.; Wan, L.-J. *Adv. Mater.* **2006**, *18*, 2426−2431. (c) Tesh, S. J.; Scott, T. B. *Adv. Mater.* **2014**, *26*, 6056−6068. (d) Ding, S.-Y.; Dong, M.; Wang, Y.-W.; Chen, Y.-T.; Wang, H.-Z.; Su, C.-Y.; Wang, W. *J. Am. Chem. Soc.* **2016**, *138*, 3031−3037.

(5) (a) He, J.; Yee, K.-K.; Xu, Z.; Zeller, M.; Hunter, A. D.; Chui, S. S.-Y.; Che, C.-M. *Chem. Mater.* **2011**, *23*, 2940−2947. (b) Liu, T.; Che, J.-X.; Hu, Y.-Z.; Dong, X.-W.; Liu, X.-Y.; Che, C.-M. *Chem. - Eur. J.* **2014**, *20*, 14090−14095. (c) Luo, F.; Chen, J. L.; Dang, L. L.; Zhou, W. N.; Lin, H. L.; Li, J. Q.; Liu, S. J.; Luo, M. B. *J. Mater. Chem. A* **2015**, *3*, 9616−9620. (d) Yee, K.-K.; Wong, Y.-L.; Zha, M.; Adhikari, R. Y.; Tuominen, M. T.; He, J.; Xu, Z. *Chem. Commun.* **2015**, *51*, 10941−10944. (e) He, F.; Wang, W.; Moon, J.-W.; Howe, J.; Pierce, E. M.; Liang, L. *ACS Appl. Mater. Interfaces* **2012**, *4*, 4373−4379. (f) Blanchard, G.; Maunaye, M.; Martin, G. *Water Res.* **1984**, *18*, 1501−1507. (g) Benhammou, A.; Yaacoubi, A.; Nibou, B.; Tanouti, B. *J. Colloid Interface Sci.* **2005**, *282*, 320−326. (h) Mon, M.; Ferrando-Soria, J.; Grancha, T.; Fortea-Pérez, F. R.; Gascon, J.; Leyva-Pérez, A.; Armentano, D.; Pardo, E. *J. Am. Chem. Soc.* **2016**, *138*, 7864−7867.

(6) (a) Mercier, L.; Detellier, C. *Environ. Sci. Technol.* **1995**, *29*, 1318−1323. (b) Moreira, W. C.; Gushikem, Y.; Nascimento, O. R. *J. Colloid Interface Sci.* **1992**, *150*, 115−120. (c) Izatt, R. M.; Bradshaw, J. S.; Bruening, R. L.; Tarbet, B. J.; Bruening, M. L. *Pure Appl. Chem.* **1995**, *67*, 1069−1074. (d) Tchinda, A. J.; Ngameni, E.; Kenfack, I. T.; Walcarius, A. *Chem. Mater.* **2009**, *21*, 4111−4121.

(7) (a) Mercier, L.; Pinnavaia, T. J. *Adv. Mater.* **1997**, *9*, 500−503. (b) Crudden, C. M.; Sateesh, M.; Lewis, R. *J. Am. Chem. Soc.* **2005**, *127*, 10045−10050. (c) Bibby, A.; Mercier, L. *Chem. Mater.* **2002**, *14*, 1591−1597. (d) Billinge, S. J. L.; McKimmy, E. J.; Shatnawi, M.; Kim, H. J.; Petkov, V.; Wermeille, D.; Pinnavaia, T. J. *J. Am. Chem. Soc.* **2005**, *127*, 8492−8498.

(8) (a) Côté, A. P.; Benin, A. I.; Ockwig, N. W.; O'Keeffe, M.; Matzger, A. J.; Yaghi, O. M. *Science* **2005**, *310*, 1166−1170. (b) Feng, X.; Ding, X.; Jiang, D. *Chem. Soc. Rev.* **2012**, *41*, 6010−6022. (c) Ding, S.-Y.; Wang, W. *Chem. Soc. Rev.* **2013**, *42*, 548−568. (d) Ascherl, L.; Sick, T.; Margraf, J. T.; Lapidus, S. H.; Calik, M.; Hettstedt, C.; Karaghiosoff, K.; Döblinger, M.; Clark, T.; Chapman, K. W.; Auras, F.; Bein, T. *Nat. Chem.* **2016**, *8*, 310−316. (e) Bunck, D. N.; Dichtel, W. R. *Angew. Chem., Int. Ed.* **2012**, *51*, 1885−1889. (f) Zeng, Y.; Zou, R.; Luo, Z.; Zhang, H.; Yao, X.; Ma, X.; Zou, R.; Zhao, Y. *J. Am. Chem. Soc.* **2015**, *137*, 1020−1023. (g) Pang, Z.-F.; Xu, S.-Q.; Zhou, T.-Y.; Liang, R.-R.; Zhan, T.-G.; Zhao, X. *J. Am. Chem. Soc.* **2016**, *138*, 4710−4713. (h) Beaudoin, D.; Maris, T.; Wuest, J. D. *Nat. Chem.* **2013**, *5*, 830−834. (i) Chandra, S.; Kandambeth, S.; Biswal, B. P.; Lukose, B.; Kunjir, S. M.; Chaudhary, M.; Babarao, R.; Heine, T.; Banerjee, R. *J. Am. Chem. Soc.* **2013**, *135*, 17853−17861. (j) Kandambeth, S.; Mallick, A.; Lukose, B.; Mane, M. V.; Heine, T.; Banerjee, R. *J. Am. Chem. Soc.* **2012**, *134*, 19524−19527.

(9) (a) Doonan, C. J.; Tranchemontagne, D. J.; Glover, T. G.; Hunt, J. R.; Yaghi, O. M. *Nat. Chem.* **2010**, *2*, 235−238. (b) Zeng, Y.; Zou, R.; Zhao, Y. *Adv. Mater.* **2016**, *28*, 2855−2873. (c) Stegbauer, L.; Hahn, M. W.; Jentys, A.; Savasci, G.; Ochsenfeld, C.; Lercher, J. A.; Lotsch, B. V. *Chem. Mater.* **2015**, *27*, 7874−7881. (d) Baldwin, L. A.; Crowe, J. W.; Pyles, D. A.; McGrier, P. L. *J. Am. Chem. Soc.* **2016**, *138*, 15134−15137.

(10) (a) Chen, L.; Furukawa, K.; Gao, J.; Nagai, A.; Nakamura, T.; Dong, Y.; Jiang, D. *J. Am. Chem. Soc.* **2014**, *136*, 9806−9809. (b) Calik, M.; Auras, F.; Salonen, L. M.; Bader, K.; Grill, I.; Handloser, M.; Medina, D. D.; Dogru, M.; Löbermann, F.; Trauner, D.; Hartschuh, A.; Bein, T. *J. Am. Chem. Soc.* **2014**, *136*, 17802−17807. (c) Du, Y.; Yang, H.; Whiteley, J. M.; Wan, S.; Jin, Y.; Lee, S.-H.; Zhang, W. *Angew.*

DOI: 10.1021/jacs.6b12885
J. Am. Chem. Soc. 2017, 139, 2786−2793

Chem., Int. Ed. **2016**, *55*, 1737−1741. (d) Bertrand, G. H. V.; Michaelis, V. K.; Ong, T.-C.; Griffin, R. G.; Dincă, M. *Proc. Natl. Acad. Sci. U. S. A.* **2013**, *110*, 4923−4928.
(11) (a) Xu, H.; Gao, J.; Jiang, D. *Nat. Chem.* **2015**, *7*, 905−912. (b) Fang, Q.; Gu, S.; Zheng, J.; Zhuang, Z.; Qiu, S.; Yan, Y. *Angew. Chem., Int. Ed.* **2014**, *53*, 2878−2882. (c) Ding, S.-Y.; Gao, J.; Wang, Q.; Zhang, Y.; Song, W.-G.; Su, C.-Y.; Wang, W. *J. Am. Chem. Soc.* **2011**, *133*, 19816−19822. (d) Peng, Y.; Hu, Z.; Gao, Y.; Yuan, D.; Kang, Z.; Qian, Y.; Yan, N.; Zhao, D. *ChemSusChem* **2015**, *8*, 3208−3212. (e) Aiyappa, H. B.; Thote, J.; Shinde, D. B.; Banerjee, R.; Kurungot, S. *Chem. Mater.* **2016**, *28*, 4375−4379. (f) Vyas, V. S.; Haase, F.; Stegbauer, L.; Savasci, G.; Podjaski, F.; Ochsenfeld, C.; Lotsch, B. V. *Nat. Commun.* **2015**, *6*, 8508. (g) Lin, S.; Diercks, C. S.; Zhang, Y.-B.; Kornienko, N.; Nichols, E. M.; Zhao, Y.; Paris, A. R.; Kim, D.; Yang, P.; Yaghi, O. M.; Chang, C. J. *Science* **2015**, *349*, 1208−1213. (h) Wang, X.; Han, X.; Zhang, J.; Wu, X.; Liu, Y.; Cui, Y. *J. Am. Chem. Soc.* **2016**, *138*, 12332−12335. (i) Sun, Q.; Aguila, B.; Perman, J. A.; Nguyen, N.; Ma, S. *J. Am. Chem. Soc.* **2016**, *138*, 15790−15796.
(12) (a) Ma, H.; Liu, B.; Li, B.; Zhang, L.; Li, Y.-G.; Tan, H.-Q.; Zang, H.-Y.; Zhu, G. *J. Am. Chem. Soc.* **2016**, *138*, 5897−5903. (b) Xu, H.; Tao, S.; Jiang, D. *Nat. Mater.* **2016**, *15*, 722.
(13) (a) Kandambeth, S.; Biswal, B. P.; Chaudhari, H. D.; Rout, K. C.; Kunjattu H., S.; Mitra, S.; Karak, S.; Das, A.; Mukherjee, R.; Kharul, U. K.; Banerjee, R. *Adv. Mater.* **2017**, *29*, 1603945. (b) Mitra, S.; Kandambeth, S.; Biswal, B. P.; Khayum M., A.; Choudhury, C. K.; Mehta, M.; Kaur, G.; Banerjee, S.; Prabhune, A.; Verma, S.; Roy, S.; Kharul, U. K.; Banerjee, R. *J. Am. Chem. Soc.* **2016**, *138*, 2823−2828. (c) Huang, N.; Ding, X.; Kim, J.; Ihee, H.; Jiang, D. *Angew. Chem.* **2015**, *127*, 8828−8831.
(14) (a) Wang, Y. Q.; Yang, C. M.; Zibrowius, B.; Spliethoff, B.; Lindén, M.; Schüth, F. *Chem. Mater.* **2003**, *15*, 5029−5035. (b) Sun, Q.; He, H.; Gao, W.-Y.; Aguila, B.; Wojtas, L.; Dai, Z.; Li, J.; Chen, Y.-S.; Xiao, F.-S.; Ma, S. *Nat. Commun.* **2016**, *7*, 13300.
(15) (a) Pramudya, Y.; Mendoza-Cortes, J. L. *J. Am. Chem. Soc.* **2016**, *138*, 15204−15213. (b) Lohse, M. S.; Stassin, T.; Naudin, G.; Wuttke, S.; Ameloot, R.; De Vos, D.; Medina, D. D.; Bein, T. *Chem. Mater.* **2016**, *28*, 626−631. (c) Nagai, A.; Guo, Z.; Feng, X.; Jin, S.; Chen, X.; Ding, X.; Jiang, D. *Nat. Commun.* **2011**, *2*, 536.
(16) Xu, F.; Xu, H.; Chen, X.; Wu, D.; Wu, Y.; Liu, H.; Gu, C.; Fu, R.; Jiang, D. *Angew. Chem., Int. Ed.* **2015**, *54*, 6814−6818.
(17) Li, B.; Zhang, Y.; Ma, D.; Shi, Z.; Ma, S. *Nat. Commun.* **2014**, *5*, 5537.
(18) (a) Sun, Q.; Dai, Z.; Liu, X.; Sheng, N.; Deng, F.; Meng, X.; Xiao, F.-S. *J. Am. Chem. Soc.* **2015**, *137*, 5204−5209. (b) Sun, Q.; Aguila, B.; Verma, G.; Liu, X.; Dai, Z.; Deng, F.; Meng, X.; Xiao, F.-S.; Ma, S. *Chem.* **2016**, *1*, 628−639.
(19) (a) Manos, M. J.; Petkov, V. G.; Kanatzidis, M. G. *Adv. Funct. Mater.* **2009**, *19*, 1087−1092. (b) Feng, X.; Fryxell, G. E.; Wang, L. Q.; Kim, A. Y.; Liu, J.; Kemner, K. M. *Science* **1997**, *276*, 923−926. (c) Bag, S.; Trikalitis, P. N.; Chupas, P. J.; Armatas, G. S.; Kanatzidis, M. G. *Science* **2007**, *317*, 490−493. (d) Shin, Y.; Fryxell, G. E.; Um, W.; Parker, K.; Mattigod, S. V.; Skaggs, R. *Adv. Funct. Mater.* **2007**, *17*, 2897−2901. (e) Yee, K.-K.; Reimer, N.; Liu, J.; Cheng, S.-Y.; Yiu, S.-M.; Weber, J.; Stock, N.; Xu, Z. *J. Am. Chem. Soc.* **2013**, *135*, 7795−7798. (f) Ai, K.; Ruan, C.; Shen, M.; Lu, L. *Adv. Funct. Mater.* **2016**, *26*, 5542−5549. (g) Abney, C. W.; Gilhula, J. C.; Lu, K.; Lin, W. *Adv. Mater.* **2014**, *26*, 7993−7997. (h) Manos, M. J.; Kanatzidis, M. G. *Chem. - Eur. J.* **2009**, *15*, 4779−4784. (i) Mon, M.; Lloret, F.; Ferrando-Soria, J.; Martí-Gastaldo, C.; Armentano, D.; Pardo, E. *Angew. Chem.* **2016**, *128*, 11333−11338.
(20) Pearson, R. G. *J. Am. Chem. Soc.* **1963**, *85*, 3533−3539.
(21) Hoffmann, G. G.; Brockner, W.; Steinfatt, I. *Inorg. Chem.* **2001**, *40*, 977−985.
(22) Lian, P.; Guo, H.-B.; Riccardi, D.; Dong, A.; Parks, J. M.; Xu, Q.; Pai, E. F.; Miller, S. M.; Wei, D.-Q.; Smith, J. C.; Guo, H. *Biochemistry* **2014**, *53*, 7211−7222.
(23) Chen, C.-C.; Mckimmy, E. J.; Pinnavaia, T. J.; Hayes, K. F. *Environ. Sci. Technol.* **2004**, *38*, 4758−4762.
(24) (a) Oh, Y.; Morris, C. D.; Kanatzidis, M. G. *J. Am. Chem. Soc.* **2012**, *134*, 14604−14608. (b) Hsi, H. C.; Rood, M. J.; Rostam-Abadi, M.; Chen, S. G.; Chang, R. *J. Environ. Eng. (Reston, VA, U. S.)* **2002**, *128*, 1080. (c) Meyer, D. E.; Meeks, N.; Sikdar, S.; Hutson, N. D.; Hua, D.; Bhattacharyya, D. *Energy Fuels* **2008**, *22*, 2290−2298. (d) Oh, Y.; Bag, S.; Malliakas, C. D.; Kanatzidis, M. G. *Chem. Mater.* **2011**, *23*, 2447−2456.

DOI: 10.1021/jacs.6b12885
J. Am. Chem. Soc. 2017, 139, 2786−2793